

Corrosion Behaviour of AZ63 Magnesium Alloy in Natural Seawater and 3.5 wt.% NaCl Aqueous Solution

Lihui Yang^{1,2,3,*}, Cunguo Lin², Haiping Gao², Weichen Xu^{1,3}, Yantao Li^{1,3}, Baorong Hou^{1,3} and Yanliang Huang^{1,3}

¹ Key Laboratory of Marine Environmental Corrosion and Bio-fouling, Institute of Oceanology, Chinese Academy of Sciences, Qingdao 266071, China

² State Key Laboratory for Marine Corrosion and Protection, Luoyang Ship Material Research Institute (LSMRI), Qingdao 266101, China

³ Open Studio for Marine Corrosion and Protection, Qingdao National Laboratory for Marine Science and Technology, Qingdao 266237, China

*E-mail: lhyang@qdio.ac.cn

Received: 23 January 2018 / Accepted: 15 May 2018 / Published: 5 July 2018

In this study, the corrosion behaviour of AZ63 magnesium alloy was investigated in natural seawater and neutral 3.5 wt.% NaCl aqueous solution. The electrochemical processes were studied using potentiodynamic polarization. The composition and morphology of the alloys and corrosion products formed were studied using X-ray diffraction (XRD) and scanning electron microscopy (SEM). The experimental results highlighted the differences between the corrosion mechanisms of AZ63 magnesium alloy in natural seawater and that in 3.5 wt.% NaCl solution. The corrosion products formed in the seawater primarily consisted of CaCO_3 and $\text{Mg}(\text{OH})_2$, while the corrosion products formed in the 3.5 wt.% NaCl solution primarily consisted of $\text{Mg}(\text{OH})_2$ and $\text{Mg}_2(\text{OH})_3\text{Cl}\cdot 4\text{H}_2\text{O}$. The results of hydrogen evolution, weight loss and potentiodynamic polarization tests showed that the AZ63 magnesium alloy samples had better corrosion resistance in natural seawater than in 3.5 wt.% NaCl aqueous solution.

Keywords: AZ63 magnesium alloy; corrosion behaviour; polarization curve; seawater

1. INTRODUCTION

Compared to other engineering metal materials (such as steel and aluminium), magnesium is an attractive metal due to a low density of $\sim 1.7 \text{ g/cm}^3$ and a relatively high abundance in the earth's crust (2.7%) and seawater (0.13%). Magnesium alloys can be widely used in many fields, such as the aerospace, electronics, and automobile industries, as well as in hydrogen energy production and

seawater-activated batteries [1,2, 11-12]. However, the poor corrosion resistance of magnesium alloys is a major obstacle to their wider application, despite high specific stiffness, good machinability, high damping capacity, castability, weldability and recyclability [2-4].

The corrosion resistance of Mg alloys is strongly affected by their composition and microstructure [5-8]. In addition to the alloy composition and microstructure, the corrosion resistance is often controlled by the degree of protection provided by the corrosion layers when exposed to chloride ion containing aqueous solutions [3, 4]. According to thermodynamic modelling, Mg^{2+} ions bind to hydroxide anions produced from the cathodic reaction. Consequently, the outer layer of corrosion products are primarily composed of $Mg(OH)_2$ [9]. There have been many studies on the electrochemical corrosion behaviour of magnesium alloys in simulated seawater, which usually employed 3.5 wt.% NaCl aqueous solution as the replacement for seawater [10-13]. However, there have been few studies investigating the corrosion behaviour of Mg alloys in natural seawater. In addition to Na^+ and Cl^- , there are many other ions in natural seawater [14], such as SO_4^{2-} , HCO_3^- , Mg^{2+} and Ca^{2+} . There have been many studies showing that the corrosion resistance and electrochemical properties are closely related to the environment because different film layers formed in different solutions [15, 16].

The aim of this work was to compare the corrosion behaviour of AZ63 Mg alloy in natural seawater with its corrosion behaviour in 3.5 wt.% NaCl aqueous solution. The corrosion behaviour of the alloy was characterized using electrochemical analysis, scanning electron microscopy (SEM), energy dispersive spectroscopy (EDS) and X-ray diffraction (XRD).

2. MATERIALS AND METHODS

The substrate materials used were AZ63 magnesium alloy samples sized 10 mm×10 mm×3 mm. The chemical composition of AZ63 magnesium alloy is shown in Table 1. Specimens were abraded with 1000 grit SiC paper to obtain an even surface, ultrasonically cleaned using acetone and washed with an alkaline detergent. The ionic composition of the natural seawater (Qingdao) is shown in Table 2. The compositions of the alloy and the seawater were measured using inductively coupled plasma mass spectrometry (ICP-MS).

Table 1. Chemical composition of AZ63 magnesium alloy

Element	Al	Zn	Cu	Ni	Mn	Si	Mg
Wt.%	5.65	2.70	0.08	0.01	0.11	0.12	Balance

Table 2. Ionic composition of the seawater (Qingdao)

Ions	Cl^-	SO_4^{2-}	HCO_3^-	Br^-	F^-	H_3BO_3	Na^+	Mg^{2+}	Ca^{2+}	K^+	Sr^{2+}
Wt.% ($\times 10^{-6}$)	18980	2649.0	139.0	64.0	1.3	26.0	10556.0	1272.0	400.0	380.0	13.3

The phases present in the AZ63 Mg alloy samples were analysed using an X-ray diffractometer (XRD, Japan Rigaku, D/max-TTR-III) with a Cu target and a monochromator, at 40 kV and 150 mA with a scanning rate of $10^\circ/\text{min}$ and a step size of 0.02° . The surface was characterized using SEM (S-3400N, Hitachi, Japan).

To evaluate the corrosion performance and possible behaviour of the samples, electrochemical measurements were performed using an electrochemical analyser (P4000+, Princeton, America). Potentiodynamic polarization tests were conducted at room temperature in natural seawater (Yellow Sea, coastal seawater from Qingdao) and neutral 3.5 wt.% NaCl aqueous solution. A standard three-compartment cell was used with a saturated calomel electrode (SCE) and a platinum electrode as a reference and a counter electrode, respectively. All of the electrodes were cleaned in acetone, agitated ultrasonically, and rinsed in deionized water before the electrochemical tests. The coated samples were masked with epoxy resins such that only 1 cm^2 was exposed to the electrolyte. During the potentiodynamic sweep experiments, the samples were first immersed in electrolyte for 10 min to stabilize the open circuit potential (OCP). The scan rate was 0.3 mV/s for all measurements. Potentiodynamic polarization tests were performed at room temperature using an electrochemical workstation in seawater and in 3.5 wt.% NaCl solution for the open circuit potential. Two parallel samples were tested for the electrochemical experiments.

A hydrogen evolution method was used to determine the corrosion rate of the magnesium alloy samples. The schematic diagram of the setup can be found in our previous work in Ref. [17]. Hydrogen gas was collected using an inverted burette and funnel above the immersed specimens. The corrosion products were removed by immersion in boiling chromic acid (20% CrO_3 + 1% AgNO_3) for 5 min. The specimens were later washed with deionised water, dried and reweighed to calculate weight loss. Three parallel samples were tested for the hydrogen evolution and mass loss tests.

3. RESULTS AND DISCUSSION

3.1. Microstructure of AZ63 magnesium alloy

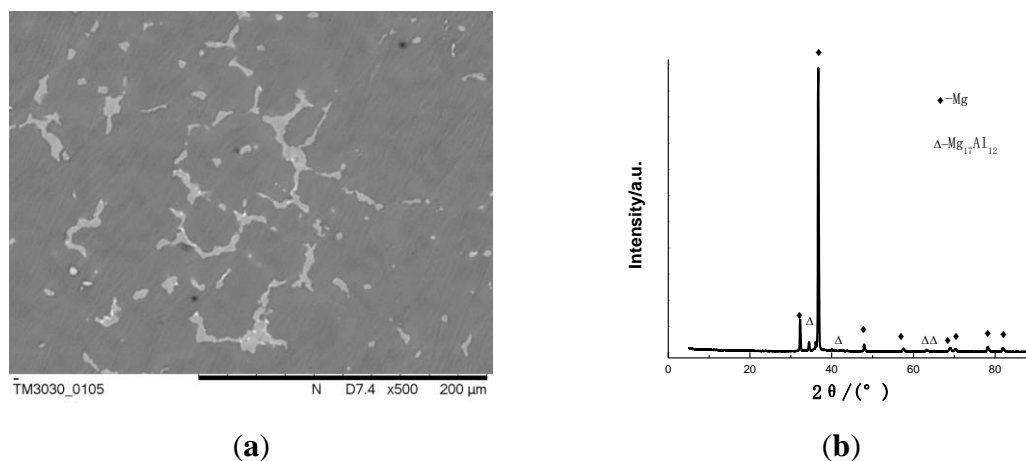


Figure 1. Optical micrograph of and XRD pattern from the unexposed AZ63 magnesium alloy sample

An optical micrograph of and XRD pattern from of the AZ63 magnesium alloy sample are shown in Figure 1. The die-cast AZ63 Mg alloy exhibited a microstructure of primary α -Mg phase and β -Mg₁₇Al₁₂ phase grains dispersed heterogeneously in the matrix [14]. The XRD results also clearly identified Mg (JCPDS No. 35-0821) and Mg₁₇Al₁₂ (JCPDS No. 73-1148) in the sample, which was consistent with the optical microstructures. The XRD results were consistent with the description of other reports [14,18].

3.2. Characterization of corrosion morphology

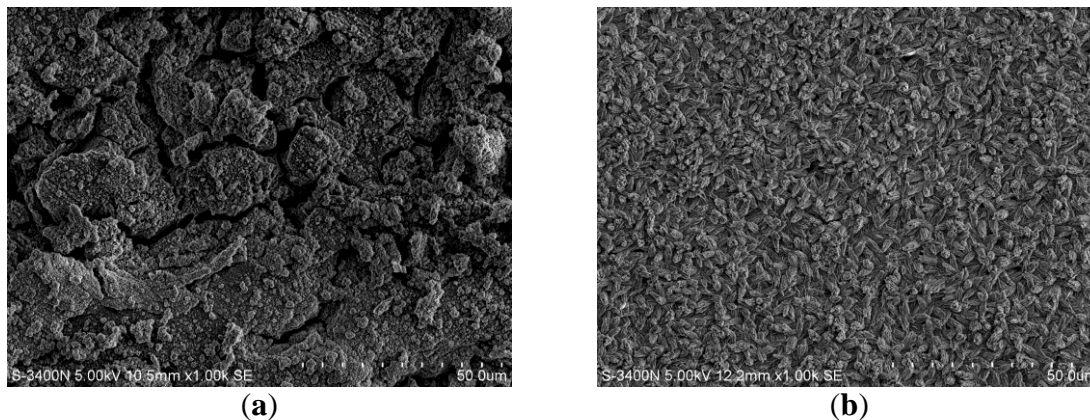


Figure 2. Corrosion morphologies of the AZ63 Mg alloy sample surfaces, with corrosion products from immersion in (a) 3.5 wt.% NaCl solution, (b) natural seawater

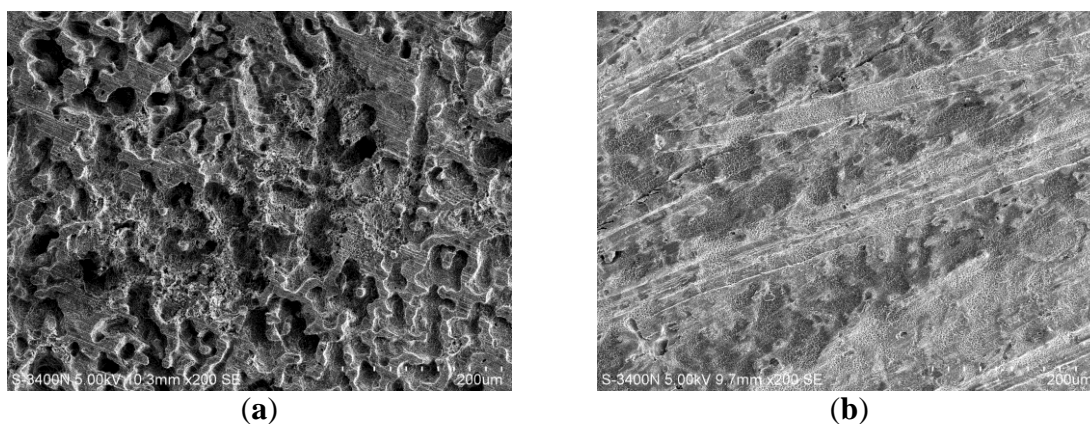


Figure 3. Corrosion morphologies of the AZ63 Mg alloy sample surfaces, with corrosion products removed after immersion in (a) 3.5 wt.% NaCl solution, (b) natural seawater

Figure 2 shows SEM of the corrosion products on the AZ63 Mg alloy sample surfaces after immersion in different solutions for 24 h. Both sample surfaces showed the growth of a large number of corrosion products. In Figure 2b, the corrosion layer produced from immersion in seawater was compact with regular deposits [19]. The corrosion layer produced from immersion in 3.5 wt.% NaCl solution was loose with many cracks (Figure 2a) [20]. After the corrosion products were removed, the

surface of the AZ63 Mg alloy sample immersed in 3.5 wt.% NaCl showed severe damage (Figure 3a). In comparison, the surface of the AZ63 Mg alloy sample immersed in seawater was relatively flat, and traces of grinding could be easily observed, as shown in Figure 3b. The results showed that the AZ63 Mg alloy samples corroded more seriously in 3.5 wt.% NaCl solutions than in seawater.

Figure 4 shows the evolution of the corrosion morphology under natural seawater immersion. Corrosion pits and deposits were seen after immersion for 6 h and 12 h. After immersion for 24 h, the surface of AZ63 magnesium alloy was almost covered by the regular and compact deposits.

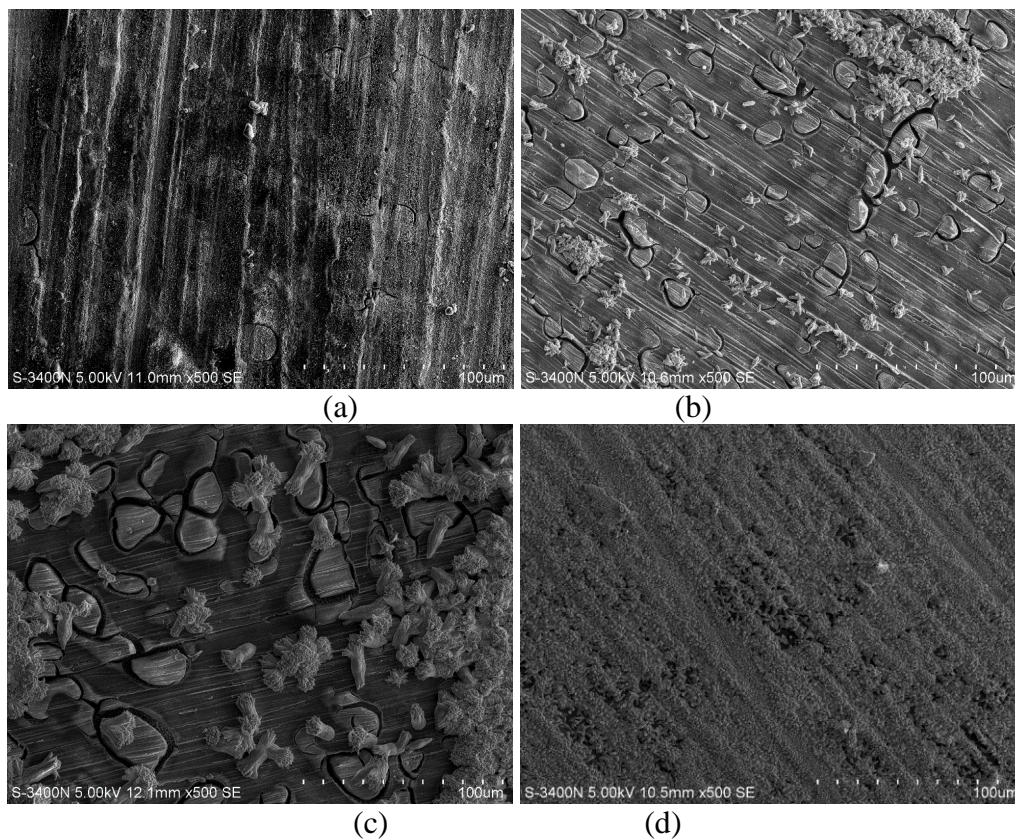


Figure 4. Corrosion morphology after immersion in seawater for (a-d): 2 h; 6 h; 12 h; 24 h

3.3 Analysis of corrosion products

The XRD patterns for the corrosion products of the AZ63 Mg alloy samples immersed in 3.5 wt.% NaCl and natural seawater are shown in Figure 5. Figure 5a shows that the corrosion products resulting from immersion in 3.5 wt.% NaCl solution primarily consisted of $\text{Mg}(\text{OH})_2$ (JCPDS No. 44-1482) and $\text{Mg}_2(\text{OH})_3\text{Cl}\cdot 4\text{H}_2\text{O}$. The Cl^- in the solution promoted corrosion of the samples and generated the more thermodynamically stable corrosion product $\text{Mg}(\text{OH})_2$ by the following equations [21]:





The reaction occurred in the solution due to the presence of Cl^{-} [22]:



In addition to $\text{Mg}(\text{OH})_2$, the corrosion products that formed in the seawater mainly consisted of CaCO_3 as shown in Figure 5b, which was determined using JCPDS card No. 24-0025. As early as several decades ago, there have been reports of calcareous deposits on the surface of carbon steel [23, 24]. The mechanism for the formation of calcium carbonate on AZ63 Mg alloy may be similar to that of carbon steel.

Due to the dissolution of Mg, hydroxyl ions concentrated near the sample surface, which changed the local region near the sample surface to an alkaline environment. The mechanism for the formation of carbonate on the surface of AZ63 magnesium alloy could be provided by the following equation [19]:

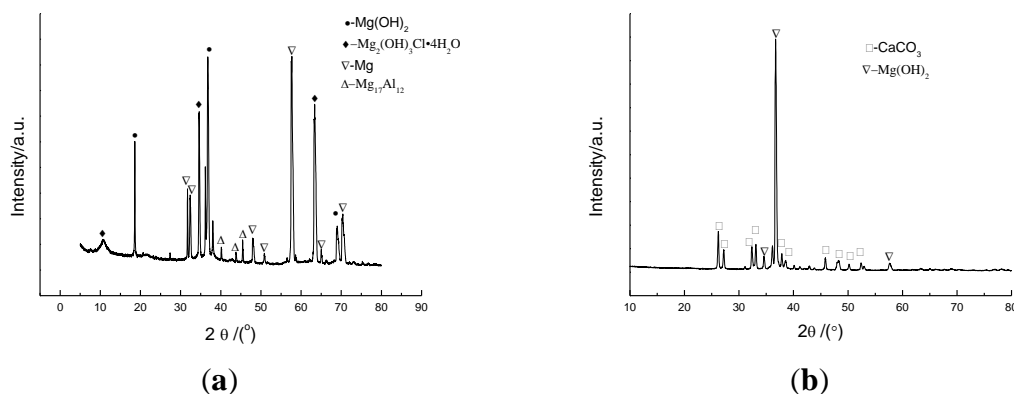
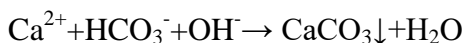


Figure 5. XRD patterns for the corrosion products resulting from immersion in (a) 3.5% NaCl solution, (b) seawater

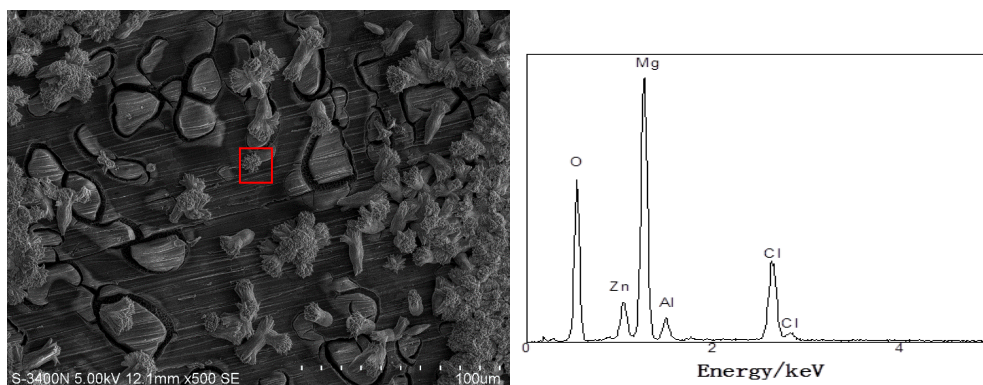


Figure 6. EDS of corrosion pits seen after immersion in seawater for 12 h

Figure 6 shows EDS of the corrosion pits seen on the sample after immersion in seawater for 12 h. EDS microprobe analyses revealed that the products in the corrosion pits were primarily composed of magnesium and oxygen, which was consistent with the XRD results that detected $Mg(OH)_2$ [25].

Figure 7 shows the EDS of the deposits observed on the sample after immersion in seawater for 12 h. The EDS microprobe analyses revealed that the cauliflower particles were primarily composed of calcium, oxygen and carbon, which was consistent with the XRD results that detected $CaCO_3$.

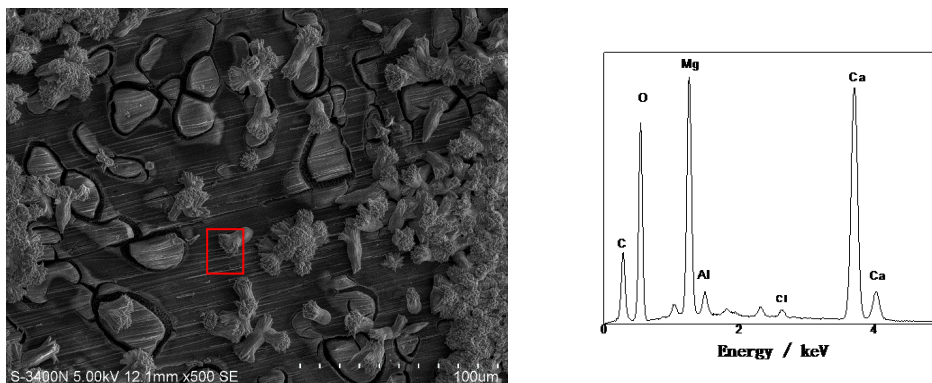


Figure 7. EDS of deposits seen after immersion in seawater for 12 h

3.4 Electrochemical results and hydrogen evolution tests

Specimens 1# and 2# were parallel samples used for *electrochemical tests in seawater*. Specimens 3# and 4# were parallel samples used for *electrochemical tests in 3.5 wt.% NaCl solution*.

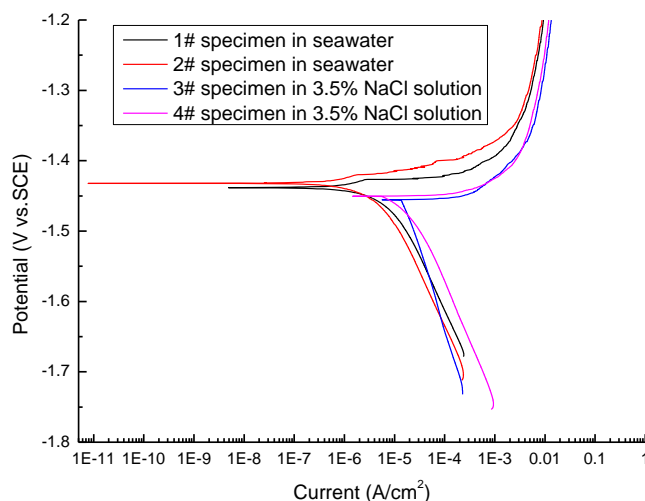


Figure 8. Potentiodynamic polarization curves for the AZ63 Mg alloy samples immersed in 3.5 wt.% NaCl solution and natural seawater

Table 3. Corrosion potential and corrosion current density values obtained from the electrochemical polarization curves

Samples	Corrosion potential, $E_{corr}(V)$		Corrosion current density, $I_{corr}(A \cdot cm^{-2})$	
1# specimen immersed in seawater	-1.438	Average value -1.436	1.828×10^{-6}	Average value 1.573×10^{-6}
2# specimen immersed in seawater	-1.433		1.317×10^{-6}	
3# specimen immersed in 3.5 wt.% NaCl solution	-1.455	Average value -1.453	1.097×10^{-5}	Average value 1.363×10^{-5}
4# specimen immersed in 3.5 wt.% NaCl solution	-1.451		1.629×10^{-5}	

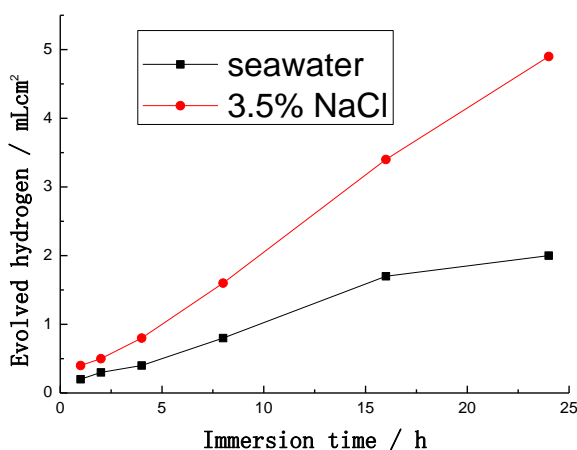


Figure 9. Hydrogen evolution rates of the AZ63 Mg alloy samples as a function of immersion time in seawater and 3.5 wt.% NaCl solution

Figure 8 shows the potentiodynamic polarization curves for the AZ63 Mg alloy samples after immersion in 3.5 wt.% NaCl solution and natural seawater for 1 h. The corrosion potential and corrosion current density values obtained from the electrochemical polarization curves are shown in Table 3. The corrosion potential of the samples exposed to seawater was approximately 17 mV lower than that of the samples exposed to 3.5 wt.% NaCl solution. The corrosion current density of the samples exposed to seawater was lower than that of the samples exposed to 3.5 wt.% NaCl solution by approximately an order of magnitude. The results revealed that the AZ63 Mg alloy samples had a greater tendency towards corrosion in 3.5 wt.% NaCl solution than in natural seawater.

The generation of hydrogen gas was accompanied by the dissolution of magnesium. The hydrogen evolution rate could directly reflect the corrosion rate of magnesium [22]. Figure 9 shows the hydrogen evolution rates of the AZ63 Mg alloy samples as a function of the immersion time in seawater and 3.5 wt.% NaCl solution. The hydrogen evolution rate measured in seawater was much lower than the rate measured in 3.5 wt.% solution. After 16 h of immersion in seawater, fewer bubbles appeared, suggesting that the reaction had slowed down and the rate of hydrogen evolution had

decreased. This finding suggests that the corrosion resistance of the AZ63 Mg alloy samples immersed in natural seawater was better than that of the samples in 3.5 wt.% NaCl solution. The weight loss of the AZ63 Mg alloy samples after immersion for 24 h in 3.5 wt.% NaCl solution was almost double the weight loss observed after exposure to natural seawater for the same time. The weight loss results were consistent with the hydrogen evolution tests.

4. CONCLUSIONS

(1) After immersion in seawater for 24 h, the corrosion products of the AZ63 Mg alloy samples primarily consisted of CaCO_3 and $\text{Mg}(\text{OH})_2$, while the corrosion products after immersion in 3.5 wt.% NaCl solution for 24 h primarily consisted of $\text{Mg}(\text{OH})_2$ and $\text{Mg}_2(\text{OH})_3\text{Cl}\cdot 4\text{H}_2\text{O}$.

(2) The corrosion potential of the samples in seawater was lower than that of the samples in 3.5 wt.% NaCl solution, and the corrosion current density of the seawater samples was also lower than that of the samples in 3.5 wt.% NaCl solution. The results indicated that AZ63 magnesium alloy corrodes more slowly in seawater than in 3.5 wt.% NaCl solution.

(3) The hydrogen evolution tests and weight loss tests were consistent with each other. The results indicated that the corrosion resistance of AZ63 Mg alloy immersed in natural seawater was better than that of the same alloy immersed in 3.5 wt.% NaCl solution, due to the compact deposits that developed on the former.

ACKNOWLEDGMENTS

The authors gratefully acknowledge the financial support of the Research Fund of State Key Laboratory for Marine Corrosion and Protection of Luoyang Ship Material Research Institute (LSMRI) under the contract No. KF160403.

References

1. M. Esmaily, J.E. Svensson, S. Fajardo, N. Birbilis, G.S. Frankel, S. Virtanen, R. Arrabal, S.Thomas, L.G. Johansson, *Prog. Mater Sci.*, 89(2017) 92.
2. G.L. Song, Corrosion Prevention of Magnesium alloys, *Woodhead Publishing: 1edition*, (2013)3.
3. G.L. Song, Corrosion of Magnesium alloys, *Woodhead Publishing Limited*, (2011)3.
4. A.Pardo, M.C. Merino, A.E. Coy, F. Viejo, F. Arrabal, Feliu Jr., *S. Electrochim. Acta*, 53(2008) 7890.
5. M.C. Delgado, F.R. García-Galvan, I. Llorante, P. Pérez, P. Adeva, S. Feliu Jr., *Corros. Sci.*, 2017, 123, 182-196.
6. S.M. Baek, H.J. Kim, H. Y. Jeong, S.D. Sohn, H.J. Shin, K.J. Choi, K.S. Lee, J.G. Lee, C.D. Yim, B.S. You, H.Y. Ha, S.S. Park, *Corros. Sci.*, 112(2016)112.
7. H.M. Jia, X.H. Feng, Y.S. Yang, *Corros. Sci.*, 120(2017)75.
8. Y.B. Hu, C. Zhang, W.Q. Meng, F.S. Pan, J.P. Zhou, *J. Alloys Compd.*, 727(2017)494.
9. H. Feng, S.H. Liu, Y. Du, T. Lei, R.C. Zeng, T.C. Yuan, *J. Alloys Compd.*, 695(2017) 2330.
10. P.W. Chu, E.L. Mire, E.A. Marquis, *Corros. Sci.*, 128(2017)253.
11. S.K. Oh, T.H. Cho, M.J. Kim, J.H. Lim, K.S. Eom, D.H. Kim, E.A. Cho, H.S. Kwon, *Int. J. Hydrogen Energy*, 42(2017)7761.

12. M. Deng, R. C. Wang, Y. Feng, N. G. Wang, L. Q. Wang, *Trans. Nonferr. Met. Soc. China*, 26(2016)2144.
13. Y. C. Shi, C. Q. Peng, Y. Feng, R.C. Wang, N.G. Wang, *Mater. Des.*, 124(2017)24.
14. J. R. Li, Q. T. Jiang, H. Y. Sun, Y.T. Li, *Corros. Sci.*, 111(2016)288.
15. Q. Jiang, X. Ma, Y. Li, K. Zhang, X. Li, B. Hou, *Mater. Sci. Technol.*, 32(2016)1613.
16. C. Taltavull, Z. Shi, B. Torres, J. Rams, A. Atrens, *J. Mater. Sci.*, 25(2014) 329.
17. L. H. Yang, J. Q. Li, Y. Z. Zheng, W. W. Jiang, M. L. Zhang. *J. Alloys Compd.*, 467 (2009) 562
18. J. R. Li, K. Wan, N. Wang, *Int. J. Electrochem. Sci.*, 12 (2017) 3030
19. B. J. Wang, D. K. Xu, J. H. Dong, W.Ke. *J. Mater. Sci. Technol.* 2018, In press
20. Sennur CANDAN, Ercan CANDAN, *Trans. Nonferr. Met. Soc. China.*, 28(2018) 642
21. G. L.Makar, J. Kruger, *Int. Mater. Rev.*,38(1993)138
22. D. Y. Chang, Y. Jie, K. W. Sang, *Corros. Sci.*,51(2009):1197
23. J.F. Yan, R.E. White, R.B. Griffin, *J. Electrochem. Soc.*, 140(1993)1275.
24. S. Elbeik, A.C.C. Tseung, A.L. Mackay, *Corros. Sci*, 26(1986) 669.
25. H. Tang , T. Wu , F.J. Xu , W. Tao , X. Jian, *Int. J. Electrochem. Sci.*, 12(2017)1377-1388

© 2018 The Authors. Published by ESG (www.electrochemsci.org). This article is an open access article distributed under the terms and conditions of the Creative Commons Attribution license (<http://creativecommons.org/licenses/by/4.0/>).